ARL-STRUC-R-425

AR-004-617

DEPARTMENT OF DEFENCE

DEFENCE SCIENCE AND TECHNOLOGY ORGANISATION

AERONAUTICAL RESEARCH LABORATORIES

MELBOURNE, VICTORIA

Structures Report 425

A FINITE ELEMENT PROCEDURE FOR INTERFERENCE-FIT AND COLD-WORKING PROBLEMS WITH LIMITED YIELDING (U)

by

R.P. CAREY and B.C. HOSKIN

DECEMBER 1986

AR-004-517

DEPARTMENT OF DEFENCE
DEFENCE SCIENCE AND TECHNOLOGY ORGANISATION
AERONAUTICAL RESEARCH LABORATORIES

Structures Report 425

A FINITE ELEMENT PROCEDURE FOR INTERFERENCE - FIT AND COLD - WORKING PROBLEMS WITH LIMITED YIELDING (U)

by

R. P. Carey and B. C. Hoskin

SUMMARY

A procedure is described for performing finite element analyses on an annular plate containing an interference-fit pin or a cold-worked hole by prescribing interface displacements. Strain-hardening is permitted but unloading beyond reverse yielding is not allowed. The procedure is verified against a comparable internal pressure case. An analytical solution for an infinite plate of a perfectly plastic material is also included for comparative purposes.

POSTAL ADDRESS: Director, Aeronautical Research Laboratories,
P.O. Box 4331, Melbourne, Victoria, 3001, Australia.

CONTENTS

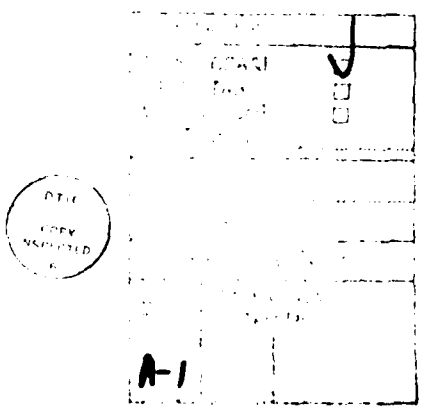

1. INTRODUCTION

Fatigue enhancement of bolt holes by methods such as interference-fitting and cold-working is a continuing research task at the Aeronuatical Research Laboratories. Part of the program involves the study of the stress/strain fields and the development of procedures for the prediction of such fields.

In a previous paper[1] the penalty finite element method was applied to the analysis of elastic two-dimensional stress/strain fields. The present paper extends the field of interest to elastic/plastic behaviour with linear strain-hardening and elastic unloading. In the process, a finite element approach has been developed in which interference is specified via relative displacements and this method has been verified against an alternative approach with internal pressure replacing the interference. In addition a further comparison with an analytical solution for an infinite plate of perfectly plastic material has been included in the Appendix.

2. FINITE ELEMENT ANALYSES

2.1. Modelling

The subject to be modelled is a simple annular aluminium alloy plate of 10:1 diameter ratio with a steel pin. The selected mesh is shown in Fig 1, only a small section having been modelled on account of radial symmetry. A fine radial sub-division of the plate mesh (into 29 elements) was considered desirable in view of the complexity of the stress/strain fields in the plastic zone and the changing position of the elastic/plastic boundary with changing loading. An 18 degree sector angle was dictated by a shape limitation for the innermost pin element whilst the division into generally four elements circumferentially was determined by interface element proportions. Quadrilateral elements were of eight-noded iso-parametric type and triangular elements were six-noded iso-parametric.

Elastic moduli of 69 GPa and 209 GPa were assumed for plate and pin with initial yield points of 480 MPa and 1720 MPa respectively. The plate material was represented by a bi-linear stress-strain law with a plastic modulus of 1200 MPa, and strain-hardening assumed isotropic. No plastic modulus was required for the pin material. The Poisson's ratios were 0.33 for the plate and 0.30 for the pin. The material properties were chosen to represent a typical aluminium alloy plate and high strength steel pin.

2.2. Prodedure

The analyses were performed on A.R.L.'s ELXSI computer using the PAFEC finite element scheme (Level 5) which performs plasticity computations using Prandtl-Reuss equations and the von Mises yield criterion. The scheme was used with modifications developed at A.R.L. to assist convergence. Two loading cases were treated as follows:

2.2.1 Interference Case

In the first case, an interference of 1.63% was introduced between pin and plate and subsequently relaxed to zero, the level selected being just below the level which would induce reverse yielding on relaxation. Plane stress conditions were adopted. The chosen interference was enforced through management of relative displacements of nodes at the interface. This was achieved by the use of a generalised constraints module of the PAFEC scheme which is able to control the displacements of nodes in terms proportional to other nodal displacements. However the characteristics of the generalised constraints module made it necessary to introduce a dummy node (separate from the main mesh) whose displacement was used as carrier for the numerical value of relative displacement and, as the relative displacement was constant around the interface, the one dummy node was used repetitively for all interface displacement relationships.

At the relaxation stage complete removal of interference was found by observing when the interface radial stress reduced to zero. The interference was applied over 46 increments and there were 21 unloading steps.

In addition to the foregoing, constraints were applied between interface node pairs such that no relative translation in the circumferential direction was permitted and in that way a bonded interface was effectively specified.

2.2.2. Internal Pressure Case

In the second case, the pin and interference fit were discarded and an internal pressure of 499.3 MPa applied to the hole in 27 increments, that pressure being the level of interface radial stress reached in the interference case. Unloading then followed in 20 steps to zero pressure. The finite element scheme represents such pressure loading by a series of point loads at nodes on the pressure face.

In comparison with the first case, additional circumferential direction restraint was required to achieve polar symmetry of stress output. Five equally-spaced radii were constrained compared with only two in the first case. Such additional restraint would not detract from the verification being undertaken.

3. RESULTS OF FINITE ELEMENT ANALYSES AND DISCUSSION

3.1. Stress and Strain Distributions

The stress and strain radial distributions found by the two methods of analysis (displacement and pressure) have been compared in the following tables:-

Table 1	1.63% Interference Stresses.
Table 2	Stresses after 1.63% cold-working.
Table 3	1.63% Interference Strains.
Table 4	Strains after 1.63% cold-working.

Perusal of Tables 1 and 2 shows that the stress distributions from the two methods are virtually identical — in the worst case a difference of 5 MPa occurs. The strain distributions, presented in Tables 3 and 4, are also consistent between methods. The maximum differences of 0.4x10-3 on radial strain and 0.2x10-3 on circumferential strain are small in relation to the peak radial and circumferential strains of 24.5x10-3 and 14.7x10-3 respectively.

Stress and strain distributions, determined by the displacement method, are depicted as follows:-

Fig.2	Stresses at 1.63% Interference.
Fig.3	Stresses after Unloading from 1.63% Interference.
Fig.4	Strains at 1.63% Interference.
Fig.5	Strains after Unloading from 1.63% Interference.
Fig.6	Von Mises Equivalent Stresses for 1.63% Interference and Unloaded Conditions.

In Figs 2 and 3 the influence of plasticity on circumferential stresses is clearly visible with quite different distribution patterns either side of the elastic/plastic boundary. The location of that boundary at a non-dimensional radial position of 1.56 is clearly seen from the slope discontinuity. Regarding the influence of plasticity on strains, Figs 4 and 5 show that the marked discontinuity in slope for circumferential stress is absent for the circumferential strain.

The equivalent stresses in Fig.6 exhibit, for the loaded state, an increasing level rising, with strain-hardening, from the initial yield point of 480 MPa at the elastic/plastic boundary to approximately 500 MPa at the hole edge. The unloaded curve shows a return to the same level of von Mises stress at the edge upon incipience of reverse yield. The existence of a marked trough is also noted.

3.2. Stresses, Strains and Displacements at the Interface

Stresses, strains and displacements at the interface have been tabulated for the loaded and unloaded states and for both interference and pressure cases as follows:-

Table 5 Stresses at the Hole Edge.

Table 6 Strains at the Hole Edge.

Table 7 Displacements at the Interface.

As already shown for the stress and strain fields, the stress and strain levels at the hole are sensibly identical for both methods. The plate displacements are also similar, differing by only about 1% at full interference and a similar absolute magnitude upon relaxation.

The circumferential stress magnitude at the hole edge was virtually negligible at the 1.63% interference level and as expected the residual stress was approximately at the current yield allowing for strain-hardening.

It is noted that the relative displacement of pin and plate at the interface agrees with the target interference level of 1.63% and that the residual deformation is 0.49% on radius.

3.3. Equivalent Stress/Strain Curve

Fig.7 shows the equivalent stress/strain curve (for the interference-fit case) for a point on the hole circumference. This curve deviates to some extent from the chosen bi-linear curve described in paragraph 2.1. Such deviation is probably caused at least in part by extrapolation to element edge nodes from the Gauss points for which computations were performed. The quality of tracking was improved by trials in which loading steps were reduced but results were fairly insensitive to tracking inaccuracy.

Comment should also be made about the unloading path on Fig.7. It initially drops from point B on the strain-hardening curve down to point C at the usual elastic slope but then reverses upwards along the same elastic line to point B again, this now being the point of incipient reverse yielding. The equivalent stress levels during elastic unloading are calculable and agree with the behaviour described.

4. ANALYTICAL SOLUTION FOR PERFECTLY PLASTIC MATERIAL

In the Appendix an analytical solution for the case when the plate material is perfectly plastic is described. Apart from ignoring work hardening, the analytical treatment also differs from the finite element one in that it is based on the Tresca, rather than the von Mises, yield criterion. This was done because simple formulae, that are of a form potentially suitable for preliminary design purposes, can then be derived; such is not the case if the von Mises criterion is used. Naturally, with these points of difference a very close agreement between the analytical and finite element results can hardly be expected. However, as is shown by the detailed comparisons made in the Appendix, there is a reasonable agreement (better than 10%, say) between the two sets of results for most of the quantities of interest (e.g. the hole expansion, the radius of the plastic regime, and the residual stresses in the vicinity of the hole). The analytical work shows that, at least for a perfectly plastic material, the onset of reversed yielding is close to the stage at which out-of-plane stresses can be expected to be developed, the problem then becoming a three-dimensional one.

5. CONCLUSIONS

(i) A displacement method for finite element analysis of interference problems has been described and verified against an alternative internal pressure method for a simple geometry of an annulus of 10:1 diameter ratio and 1.63% interference level. The method should be applicable also at other interference levels.

(ii) For the case of a steel pin in a plate of typical aluminium alloy 1.63% interference is the level beyond which reverse yield will occur on relaxation. At that interference the circumferential stress was small, but on a relaxation the stress as expected attained the level of 503 MPa (compressive) corresponding to the current yield point. A permanent hole enlargement of 0.49% resulted from this interference.

(iii) The analytical solution for a perfectly plastic material, given in the Appendix shows sufficient agreement with the finite element one to indicate that, as long as the degree of work hardening is comparable with that of the present example, the analytical solution should be useful for preliminary design studies.

(iv) The discussion in the Appendix also indicates that three-dimensional effects are likely to become important if the problem is pursued significantly beyond the threshold of reverse plasticity.

6. FUTURE PROPOSALS

(i) It is desirable to simulate cold-working to higher, more representative, levels at which reverse yielding takes place. Three-dimensional finite element analysis will probably be necessary.

(ii) A capability for kinematic hardening on reverse yielding would enable simulation of the Bauschinger Effect.

(iii) The displacement method should be applicable to interference-fitting and cold-working problems involving non-axisymmetric geometries, such as a bolt near an edge of closely spaced bolts.

7. ACKNOWLEDGEMENTS

The authors wish to acknowledge information provided by Mr N. S. Swansson regarding modification of the finite element scheme and the interest shown in the investigation by Drs R. Jones, G. S. Jost, and A. Wong.

REFERENCES

1. Heller, M., Paul, J., Carey, R. P. and Jones, R. "Finite Element Analysis of Problems associated with Life Enhancement Techniques", A.R.L. Structures Report 404, June, 1984.

2. Koiter, W. T. On partially plastic thick walled tubes, pp 233–251 of "Anniversary Volume on Applied Mechanics dedicated to C. B. Biezeno", N. V. De Technische Uitgeverij H. Stam, 1953.

APPENDIX

COMPARISON OF FINITE ELEMENT WITH ANALYTICAL SOLUTION FOR A PERFECTLY PLASTIC MATERIAL

A1 GENERAL

In this Appendix an analytical solution for the radial expansion of a circular hole in an infinite plate by an internal pressure is cited for the purpose of comparison with the preceding finite element results. This solution is for a perfectly plastic (i.e. non-work hardening) material obeying the Tresca yield condition and associated flow rule; it is derived from the work of Koiter (ref. 2) on the more complicated case of a thick-walled tube under internal pressure. As in the finite element treatment, plane stress conditions are assumed.

A2 NOTATION

r	radial co-ordinate
R	radius of hole
ρ	radius of elastic-plastic boundary
z	co-ordinate perpendicular to plane of plate
u	radial displacement
e_{rr}	radial strain
$e_{\theta\theta}$	circumferential strain
e_{zz}	out-of-plane strain
T_{rr}	radial stress
$T_{\theta\theta}$	circumferential stress
T_{zz}	out-of-plane stress (zero for plane stress)
p	applied pressure
Y	uniaxial yield stress; see also Section A7
E	Young's modulus
ν	Poisson's ratio

A3 OUTLINE OF ANALYSIS

The problem under consideration is shown in Fig.8. Because of the radial symmetry the radial, circumferential and out-of-plane directions are those of the principal stresses and the sole equilibrium condition is

$$\frac{dT_{rr}}{dr} + \frac{T_{rr} - T_{\theta\theta}}{r} = 0 \tag{1}$$

with the strain-displacement relations being

$$e_{rr} = \frac{du}{dr} \quad , \quad e_{\theta\theta} = \frac{u}{r} \tag{2}$$

In the plastic region Tresca's yield condition applies i.e.,

$$\text{maximum modulus of } \{ T_{\theta\theta} - T_{rr},\ T_{rr} - T_{zz},\ T_{zz} - T_{\theta\theta} \} = Y \tag{3}$$

With $T_{zz}=0$, and from a knowledge of the purely elastic solution where $T_{\theta\theta} > 0$ and $T_{rr} < 0$, it follows that in the initial stages of yielding the condition (3) reduces to

$$T_{\theta\theta} - T_{rr} = Y \tag{4}$$

(As will be discusssed later this condition is only valid up to a certain applied pressure, namely $p = Y$, and indeed, the solution given here is only valid to that same pressure)

Using eqns (1) and (4), and applying the boundary condition

$$r = R \ , \ T_{rr} = -p \tag{5}$$

the stresses in the plastic region are readily determined:

$$R \leq r \leq \rho \qquad T_{rr} = -p + Y \ln(r/R) \tag{6a}$$

$$T_{\theta\theta} = Y - p + Y \ln(r/R) \tag{6b}$$

In the elastic region, Hooke's law applies; for plane stress conditions this takes the form

$$E\, e_{rr} = T_{rr} - \nu T_{\theta\theta} \tag{7a}$$

$$E\, e_{\theta\theta} = T_{\theta\theta} - \nu T_{rr} \tag{7b}$$

$$E\, e_{zz} = -\nu(T_{rr} + T_{\theta\theta}) \tag{7c}$$

Using eqns (1), (2), (7a) and (7b) in conjunction with the boundary conditions

$$r \to \infty \quad , \quad u \to 0 \tag{8}$$

$$r = \rho \quad , \quad T_{\theta\theta} - T_{rr} = Y \tag{9}$$

gives the displacement, strains and stresses in the elastic region. (The condition (9) is the requirement that on the boundary of the elastic and plastic regions, the stresses as determined in the elastic region must also satisfy the yield condition).
The results are as follows:

$$r \geq \rho \qquad u = \frac{(1+\nu)Y}{2E}\,\frac{\rho^2}{r} \tag{10a}$$

$$e_{rr} = \frac{-(1+\nu)Y}{2E}\,\frac{\rho^2}{r^2} \quad , \quad e_{\theta\theta} = \frac{(1+\nu)Y}{2E}\,\frac{\rho^2}{r^2} \tag{10b}$$

$$T_{rr} = \frac{-Y}{2}\,\frac{\rho^2}{r^2} \quad , \quad T_{\theta\theta} = \frac{Y}{2}\,\frac{\rho^2}{r^2} \tag{10c}$$

The radius of the elastic-plastic boundary is determined by the requirement that the radial stress must be continuous across it. Thus, equating eqn (6a) and the first of eqns (10c) gives:

$$p = Y\{1/2 + \ln(\rho/R)\} \tag{11a}$$

or

$$\rho/R = \exp\{(2p - Y)/2Y\} \tag{11b}$$

Incidentally the above shows that yielding commences (naturally on the hole boundary) when $p = Y/2$. It only remains to calculate the displacement and strains in the plastic region. As shown by Koiter, as long as the out-of-plane stress is the intermediate principal stress, the general requirement that the plastic strain increment vector must be normal to the yield surface can be used to establish that the plastic component of the out-of-plane strain is zero; the only component is the elastic one which is given by

$$E\,e_{zz} = -\nu(T_{rr} + T_{\theta\theta}) \tag{12}$$

Thus, the volumetric expansion in the plastic region is

$$e_{rr} + e_{\theta\theta} + e_{zz} = \frac{du}{dr} + \frac{u}{r} - \frac{\nu}{E}(T_{rr} + T_{\theta\theta}) \tag{13}$$

and, since plastic straining is incompressible, the volumetric expansion is related to the hydrostatic component of the stresses by the usual elastic formula. Thus, it follows that

$$T_{rr} + T_{\theta\theta} = \frac{E}{(1-2\nu)}\left\{\frac{du}{dr} + \frac{u}{r} - \frac{\nu}{E}(T_{rr} + T_{\theta\theta})\right\} \tag{14}$$

On substituting for the stresses from eqn (6) and solving the resultant differential equation, with the boundary condition,

$$r = \rho \ , \ u = \frac{(1+\nu)Y\rho}{2E} \tag{15}$$

(which follows from the requirement that the displacement must be continuous across the elastic-plastic boundary) it can be established after a little algebra that the displacement is given by

$$u = \frac{(1-\nu)Yr}{E}\left[\frac{p}{Y}\left(\frac{\rho^2}{r^2} - 1\right) + \frac{(1+\nu)}{(1-\nu)}\,\frac{\rho^2}{2r^2} + \ln(r/R) - \frac{\rho^2}{r^2}\ln(\rho/R)\right] \tag{16}$$

Using eqn (11a) this can be simplified somewhat and the strains can, of course, be calculated from eqns (2).
The results are:

$$R \leq r \leq \rho \qquad u = \frac{(1-\nu)Yr}{E}\left[-\frac{p}{Y} + \ln\frac{r}{R} + \frac{1}{1-\nu}\frac{\rho^2}{r^2}\right] \tag{17a}$$

$$e_{rr} = \frac{(1-\nu)Y}{E}\left[-\frac{p}{Y} + 1 + \ln\frac{r}{R} - \frac{1}{1-\nu}\frac{\rho^2}{r^2}\right] \tag{17b}$$

$$e_{\theta\theta} = \frac{(1-\nu)Y}{E}\left[-\frac{p}{Y} + \ln\frac{r}{R} + \frac{1}{1-\nu}\frac{\rho^2}{r^2}\right] \tag{17c}$$

A4 LIMIT OF VALIDITY OF SOLUTION

The present (plane stress) solution is only valid as long as the radial stress at the hole is less than or equal to the yield stress, i.e. up to

$$T_{rr}(R) = -p = -Y \tag{18}$$

For values of p greater than Y it is only possible to satisfy the yield condition

$$\text{modulus of } \{ T_{rr}(R) - T_{zz}(R) \} \leq Y$$

with non-zero T_{zz}. Thus, for $p > Y$ it must be anticipated that out-of-plane stresses will be developed. (This, of course, is consistent with the experimental observation that raised lips are developed around holes which undergo substantial cold-expansion.) The resultant three-dimensional problem is vastly more difficult and recourse to numerical methods (e.g. ref.1) would seem necessary.

A5 PRESSURE DUE TO INTERFERENCE—FIT BOLT

When the pressure on the hole surface is developed by an interference-fit bolt, with the degree of interference prescribed, then the associated pressure can be determined as follows. Assuming that the degree of interference is sufficient to cause yielding of the plate but not of the bolt, the radial expansion of the hole boundary as given by eqn (17a) is

$$u(R) = \frac{(1-\nu)YR}{E}\left[-\frac{p}{Y} + \frac{1}{1-\nu}\frac{\rho^2}{r^2}\right]$$

or, using eqn (11b)

$$u(R) = \frac{(1-\nu)YR}{E}\left[-\frac{p}{Y} + \frac{1}{1-\nu}\exp\{(2p-Y)/Y)\}\right] \tag{19}$$

If E_B and ν_B denote Young's modulus and Poisson's ratio for the bolt material, then the radial displacement u_B, of the bolt boundary is given by the standard formula

$$u_B = -p\frac{(1-\nu_B)}{E_B}R \tag{20}$$

Denoting by δ the amount by which the radius of the bolt initially exceeds that of the hole, then the interference-fit requirement is that

$$u(R) - u_B = \delta \tag{21}$$

On substituting from eqns (19) and (20) into (21), the required equation for p is obtained.
The limiting value of interference, δ_L, beyond which the present solution is not valid can be obtained by setting $p = Y$ in eqn (21). The result can be written in the form

$$\frac{\delta_L}{R} = \frac{Y(1-\nu)}{E}\left[\frac{e}{1-\nu} - 1 + \frac{(1-\nu_B)}{(1-\nu)}\frac{E}{E_B}\right] \qquad (22)$$

where e here denotes the exponential constant.

A6 RESIDUAL STRESSES

When the applied pressure, p, is removed from the hole surface, and with the proviso that reversed yielding does not occur, the residual stresses, strains and displacements in the plate can be determined simply by subtracting from the previously obtained values, the corresponding values as given by the purely elastic solution for an applied pressure p. Thus the residual stresses are obtained by subtracting from eqns (6) and *(10c) the values*

$$T^*_{rr} = -pR^2/r^2 \quad , \quad T^*_{\theta\theta} = pR^2/r^2 \qquad (23)$$

Likewise the residual strains are obtained by subtracting from eqns (17b and c) and (10b) the values

$$e^*_{rr} = -p\frac{(1+\nu)}{E}\frac{R^2}{r^2} \quad , \quad e^*_{\theta\theta} = p\frac{(1+\nu)}{E}\frac{R^2}{r^2} \qquad (24)$$

Finally, the residual displacements are determined by subtracting from eqns (17a) and (10a) the value

$$u^* = \frac{p(1+\nu)}{E}\frac{R^2}{r} \qquad (25)$$

From a consideration of eqns (6) and (23) for r = R, it is readily established that p = Y defines the load causing incipient reversed yielding.

A7 COMPARISON WITH FINITE ELEMENT SOLUTION

Here the above analytical results are compared with the finite element results obtained in the body of the report. Points of difference between the two models are, firstly, that the analytical work has been for a perfectly plastic material obeying Tresca's yield condition and associated flow rule, whilst the finite element work was for a work-hardening material obeying the von Mises yield condition and the Prandtl-Reuss flow rule. As can be seen from Fig. 7 the degree of work hardening is relatively small in the present case, so it might be hoped that large differences would not result from this cause. Differences associated with the use of the Tresca, rather than the von Mises, yield condition warrant further discussion. For the present problem the von Mises condition reduces to

$$T_{\theta\theta}^2 - T_{rr}T_{\theta\theta} + T_{rr}^2 = Y^2 \qquad (26)$$

This gives the ellipse shown in Fig.9 Also shown in Fig.9 is the Tresca hexagon corresponding to *the yield condition used in the analysis, namely,*

$$\text{maximum modulus of } \{ T_{\theta\theta} - T_{rr} \ , \ T_{\theta\theta} \ , \ T_{rr} \} = Y \qquad (27)$$

It can be seen that this hexagon and the ellipse coincide at the corners of the hexagon; in particular there is agreement for yielding under uniaxial loads. However, in the present problem the stress history of a point on the boundary of the hole (for a perfectly plastic von Mises material) would be des-

cribed by the path OAB on Fig.9; other points in the plastic region follow the same path but do not reach B. There is a considerable discrepancy between the (inscribed) hexagon and the ellipse in the vicinity of point A, corresponding to the fact that the von Mises criterion predicts that the yield stress in shear is $1/\sqrt{3}$ times that in tension, whilst the corresponding factor for the Tresca criterion is 1/2. Suppose, now, that Y in eqn (27) is replaced by $2Y/\sqrt{3} = 1.154Y$; then, as shown on Fig.9, the resulting Tresca hexagon circumscribes the ellipse and the point A lies on both the hexagon and the ellipse. However, the previous coincidence at point B is now lost In an inituitive attempt to minimise the maximum error, at least approximately, here the quantity Y in eqn (27) will be replaced by 1.077Y corresponding to a hexagon that lies midway between those shown in Fig.9.

A second point of difference between the analytical and the finite element work is that the former deals with a plate of infinite extent whilst the latter deals with an annulus having a 10:1 diameter ratio, but this should have little effect on the quantities of interest.

The following are the values of the material constants used in the comparison:

	Plate	Bolt
E (GPa)	69	209
ν	0.33	0.30
Y(MPa)	517*	—

(*This value is 480 x 1.077, in accord with the discussion given earlier).

The finite element results have all been for the case when the maximum load applied to the hole is such as to cause incipient reversed yielding on unloading. The analytical results have also been presented for this case. As discussed in Section A6 this corresponds to p=Y=517MPa. The corresponding finite element value is p = 500MPa (Table 1).

(a) Hole expansion

The hole expansion at maximum load, as obtained from eqn (19) with p = Y is u/R = 1.54%; the corresponding FE value from Table 7 is 1.45%. The residual hole expansion after load removal, as obtained by subtracting from the above value, the value given by eqn (25) with p = Y is 0.54%; the FE value from Table 7 is 0.47%.

(b) Limiting interference fit

The limiting value of the interference fit, from eqn (22), is 1.71%; the FE value is 1.63%.

(c) Elastic-plastic boundary

The radius of the elastic-plastic boundary as obtained from eqn (11b) with ρ = y is 1.65 R; the FE value, as read from Fig.2, is 1.56 R.

(d) Stresses and residual stresses

The radial and circumferential stresses as given by the analytical solution with p = Y have been shown in Fig. 10 and the residual stresses after unloading have been shown in Fig. 11; in each case the stresses have been plotted in the form T/Y. Also shown in these Figures are representative points from the FE solution; these have been obtained by dividing the values given in Tables 1 and 2 by Y = 517.

(e) Strains and residual strains

In an analogous fashion the strains and the residual strains are shown in Figs 12 and 13.

A8 DISCUSSION

As can be seen from the foregoing, there is a reasonable agreement (better than 10%, say) between the analytical and FE values, for many of the quantities of interest. This is the case for the maximum value of the load and the hole expansion, for the limiting value of the interference fit leading to reversed yielding on unloading, and the radius of the elastic-plastic boundary. There is also a generally good agreement in the stress and residual stress distributions, with the exception that circumferential stresses in the vicinity of the elastic-plastic boundary are somewhat higher in the FE case. Likewise, there is a generally good agreement in the strain and residual strain distributions; one exception is the radial strain at the hole boundary where the FE value exceeds the analytical value by almost 20%.

From the foregoing it is concluded, that provided t' unt of work-hardening is comparable with that in the FE example, the above analytical sol : a perfectly plastic material should be useful for preliminary design studies.

Finally, it is again emphasized that the analytical solution is only valid as long as the pressure on the hole surface does not exceed the yield stress; beyond that, out-of-plane stresses will be developed.

TABLE 1. 1.63% INTERFERENCE STRESSES—PLANE STRESS

RADIAL POSITION (NON-DIMENSIONAL)	STRESSES (MPA) DISPLACEMENT METHOD		PRESSURE METHOD	
	CIRCUM	RADIAL	CIRCUM	RADIAL
1.000	6.	-499.	6.	-500.
1.015	16.	-493.	17.	-493.
1.029	26.	-487.	28.	-485.
1.044	37.	-479.	39.	-478.
1.058	47.	-472.	49.	-471.
1.073	58.	-465.	59.	-464.
1.087	68.	-458.	69.	-457.
1.102	77.	-451.	79.	-450.
1.116	87.	-444.	89.	-443.
1.140	101.	-433.	104.	-432.
1.163	115.	-422.	118.	-421.
1.192	132.	-409.	135.	-408.
1.221	148.	-396.	152.	-394.
1.250	164.	-383.	167.	-382.
1.279	179.	-370.	182.	-369.
1.314	195.	-356.	199.	-354.
1.349	212.	-341.	215.	-340.
1.396	231.	-323.	235.	-321.
1.442	250.	-304.	255.	-302.
1.501	271.	-283.	272.	-281.
1.559	283.	-261.	280.	-259.
1.617	256.	-243.	254.	-241.
1.675	238.	-225.	236.	-224.
1.734	223.	-210.	222.	-209.
1.792	209.	-196.	208.	-195.
1.850	197.	-184.	196.	-183.
1.908	185.	-172.	184.	-171.
1.966	175.	-162.	174.	-161.
2.025	165.	-152.	164.	-151.
2.083	157.	-144.	156.	-143.
2.141	148.	-135.	147.	-134.
2.199	141.	-128.	140.	-127.
2.257	134.	-121.	133.	-120.
2.316	128.	-115.	127.	-114.
2.374	122.	-109.	121.	-108.
2.432	117.	-104.	116.	-103.
2.490	111.	-98.	111.	-98.
2.549	107.	-94.	106.	-93.
2.607	102.	-89.	102.	-89.
2.665	98.	-85.	98.	-85.
2.723	94.	-81.	94.	-81.
2.810	89.	-76.	88.	-76.
2.898	84.	-71.	83.	-70.
3.072	76.	-63.	75	-62.
3.247	68.	-55.	67.	-54.
3.480	61.	-48.	60.	-47.

TABLE 2. STRESSES AFTER 1.63% COLD—WORKING PLANE STRESS

RADIAL POSITION (NON-DIMENSIONAL)	STRESSES (MPA)			
	DISPLACEMENT METHOD		PRESSURE METHOD	
	CIRCUM	RADIAL	CIRCUM	RADIAL
1.000	-502.	-1.	-505.	-0.
1.015	-479.	-9.	-479.	-6.
1.029	-455.	-16.	-454.	-13.
1.044	-431.	-22.	-431.	-19.
1.058	-408.	-27.	-407.	-25.
1.073	-385.	-32.	-385.	-30.
1.087	-363.	-37.	-363.	-34.
1.102	-343.	-41.	-342.	-38.
1.116	-322.	-45.	-321.	-43.
1.140	-292.	-50.	-291.	-48.
1.163	-262.	-55.	-260.	-53.
1.192	-228.	-59.	-226.	-57.
1.221	-194.	-63.	-192.	-61.
1.250	-164.	-66.	-162.	-63.
1.279	-133.	-68.	-131.	-66.
1.314	-101.	-69.	-99.	-67.
1.349	-70.	-70.	-67.	-67.
1.396	-33.	-69.	-30.	-66.
1.442	3.	-68.	8.	-65.
1.501	42.	-64.	42.	-61.
1.559	71.	-59.	68.	-57.
1.617	58.	-55.	56.	-53.
1.675	54.	-51.	52.	-49.
1.734	51.	-48.	49.	-46.
1.792	47.	-44.	45.	-43.
1.850	45.	-42.	43.	-40.
1.908	42.	-39.	40.	-37.
1.966	40.	-37.	38.	-35.
2.025	37.	-34.	36.	-33.
2.083	35.	-33.	34.	-31.
2.141	34.	-31.	32.	-29.
2.199	32.	-29.	31.	-28.
2.257	30.	-27.	29.	-26.
2.316	29.	-26.	28.	-25.
2.374	28.	-25.	27.	-24.
2.432	26.	-23.	25.	-23.
2.490	25.	-22.	24.	-21.
2.549	24.	-21.	23.	-20.
2.607	23.	-20.	22.	-19.
2.665	22.	-19.	21.	-19.
2.723	21.	-18.	20.	-18.
2.810	20.	-17.	19.	-17.
2.898	19.	-16.	18.	-15.
3.072	17.	-14.	16.	-14.
3.247	15.	-12.	15.	-12.
3.480	14.	-11.	13.	-10.

TABLE 3. 1.63% INTERFERENCE STRAINS—PLANE STRESS

RADIAL POSITION (NON-DIMENSIONAL)	STRAINS (X10-3) DISPLACEMENT METHOD		PRESSURE METHOD	
	CIRCUM	RADIAL	CIRCUM	RADIAL
1.000	14.7	-24.5	14.5	-24.2
1.015	14.1	-23.3	14.0	-23.0
1.029	13.6	-22.1	13.4	-21.7
1.044	13.1	-21.0	13.0	-20.7
1.058	12.6	-20.0	12.5	-19.6
1.073	12.2	-19.0	12.1	-18.7
1.087	11.8	-18.1	11.7	-17.8
1.102	11.4	-17.3	11.3	-17.0
1.116	11.0	-16.5	10.9	-16.2
1.140	10.5	-15.4	10.4	-15.1
1.163	9.9	-14.2	9.9	-14.0
1.192	9.4	-13.1	9.3	-12.9
1.221	8.8	-12.0	8.8	-11.8
1.250	8.4	-11.1	8.3	-10.9
1.279	7.9	-10.2	7.9	-10.0
1.314	7.5	-9.3	7.4	-9.2
1.349	7.0	-8.5	7.0	-8.3
1.396	6.6	-7.5	6.5	-7.4
1.442	6.1	-6.6	6.1	-6.5
1.501	5.6	-5.8	5.6	-5.7
1.559	5.2	-5.0	5.2	-5.0
1.617	4.9	-4.7	4.8	-4.7
1.675	4.5	-4.4	4.5	-4.4
1.734	4.2	-4.1	4.2	-4.1
1.792	4.0	-3.8	3.9	-3.8
1.850	3.7	-3.6	3.7	-3.6
1.908	3.5	-3.4	3.5	-3.4
1.966	3.3	-3.2	3.3	-3.2
2.025	3.1	-3.0	3.1	-3.0
2.083	3.0	-2.8	2.9	-2.8
2.141	2.8	-2.7	2.8	-2.7
2.199	2.7	-2.5	2.6	-2.5
2.257	2.5	-2.4	2.5	-2.4
2.316	2.4	-2.3	2.4	-2.3
2.374	2.3	-2.2	2.3	-2.1
2.432	2.2	-2.1	2.2	-2.0
2.490	2.1	-2.0	2.1	-1.9
2.549	2.0	-1.9	2.0	-1.9
2.607	1.9	-1.8	1.9	-1.8
2.665	1.8	-1.7	1.8	-1.7
2.723	1.8	-1.6	1.7	-1.6
2.810	1.7	-1.5	1.6	-1.5
2.898	1.6	-1.4	1.5	-1.4
3.072	1.4	-1.3	1.4	-1.3
3.247	1.2	-1.1	1.2	-1.0
3.480	1.1	-1.0	1.1	-1.0

TABLE 4 STRAINS AFTER 1.63% COLD—WORKING PLANE STRESS

RADIAL POSITION (NON-DIMENSIONAL)	STRAINS (X10–3) DISPLACEMENT METHOD		PRESSURE METHOD	
	CIRCUM	RADIAL	CIRCUM	RADIAL
1.000	4.9	–14.8	4.7	–14.5
1.015	4.6	–13.9	4.4	–13.6
1.029	4.4	–13.0	4.2	–12.6
1.044	4.1	–12.2	4.0	–11.8
1.058	3.9	–11.3	3.7	–11.0
1.073	3.7	–10.6	3.6	–10.3
1.087	3.5	–9.9	3.4	–9.6
1.102	3.4	–9.3	3.2	–9.0
1.116	3.2	–8.7	3.0	–8.4
1.140	3.0	–7.9	2.8	–7.6
1.163	2.7	–7.1	2.6	–6.8
1.192	2.5	–6.3	2.4	–6.1
1.221	2.3	–5.6	2.2	–5.3
1.250	2.1	–4.9	2.0	–4.7
1.279	2.0	–4.3	1.9	–4.1
1.314	1.8	–3.7	1.7	–3.6
1.349	1.7	–3.2	1.6	–3.0
1.396	1.5	–2.6	1.5	–2.5
1.442	1.4	–2.0	1.3	–1.9
1.501	1.3	–1.5	1.2	–1.4
1.559	1.2	–1.1	1.1	–1.0
1.617	1.1	–1.1	1.1	–1.0
1.675	1.0	–1.0	1.0	–1.0
1.734	1.0	–.9	.9	–.9
1.792	.9	–.9	.9	–.8
1.850	.8	–.8	.8	–.8
1.908	.8	–.8	.8	–.7
1.966	.7	–.7	.7	–.7
2.025	.7	–.7	.7	–.7
2.083	.7	–.6	.6	–.6
2.141	.6	–.6	.6	–.6
2.199	.6	–.6	.6	–.6
2.257	.6	–.5	.5	–.5
2.316	.5	–.5	.5	–.5
2.374	.5	–.5	.5	–.5
2.432	.5	–.5	.5	–.4
2.490	.5	–.4	.5	–.4
2.549	.5	–.4	.4	–.4
2.607	.4	–.4	.4	–.4
2.665	.4	–.4	.4	–.4
2.723	.4	–.4	.4	–.4
2.810	.4	–.3	.4	–.3
2.810	.4	–.3	.4	–.3
2.898	.4	–.3	.3	–.3
3.072	.3	–.3	.3	–.3
3.247	.3	–.3	.3	–.2
3.480	.2	–.2	.2	–.2

TABLE 5

STRESSES AT HOLE EDGE UNDER INTERFERENCE—FIT AND PRESSURE LOADING AND UPON RELAXATION

	LOADING	METHOD	STRESS (MPa)[1] CIRCUM	RADIAL
PLATE	1.63% INTERFERENCE	DISPLACEMENT	6.3	-499.0
	499.3 MPa	PRESSURE	5.5	-499.6
	UNLOADED	DISPLACEMENT	-503.0[2]	0.0[2]
		PRESSURE	-504.2	0.0

Notes:

1. These are average values for similar nodes, the ranges being in each case within ± 0.6 MPa.
2. Interpolation between increments was used to obtain these values.

TABLE 6

STRAINS AT HOLE EDGE UNDER INTERFERENCE—FIT AND PRESSURE LOADING AND UPON RELAXATION

	LOADING	METHOD	STRAINS (x10–3)[1] CIRCUM	RADIAL
PLATE	1.63% INTERFERENCE	DISPLACEMENT	14.6	–24.4
	499.3 MPa	PRESSURE	14.5	–24.2
	UNLOADED	DISPLACEMENT	–4.9[2]	–14.8[2]
		PRESSURE	4.7	–14.5

Notes:

1. Strains from node to node around the interface were consistent within ± 0.04x10–3
2. Interpolation *between increments* was used to obtain these values.

TABLE 7

DISPLACEMENTS AT INTERFACE UNDER INTERFERENCE—FIT AND PRESSURE LOADING AND UPON RELAXATION

		DISPLACEMENTS (%)[1]		
LOADING	METHOD	PLATE	PIN	RELATIVE
1.63% INTERFERENCE	DISPLACEMENT	1.46%	-0.17%	1.63%[2]
499.3 MPa	PRESSURE	1.45%	-	-
UNLOADED	DISPLACEMENT	0.49%[3]	0.0[3]	
	PRESSURE	0.47%	-	-

Note:

1. Expressed as a percentage of radius.
2. This relative displacement matches the target interference.
3. Interpolation between increments was used to obtain these values.

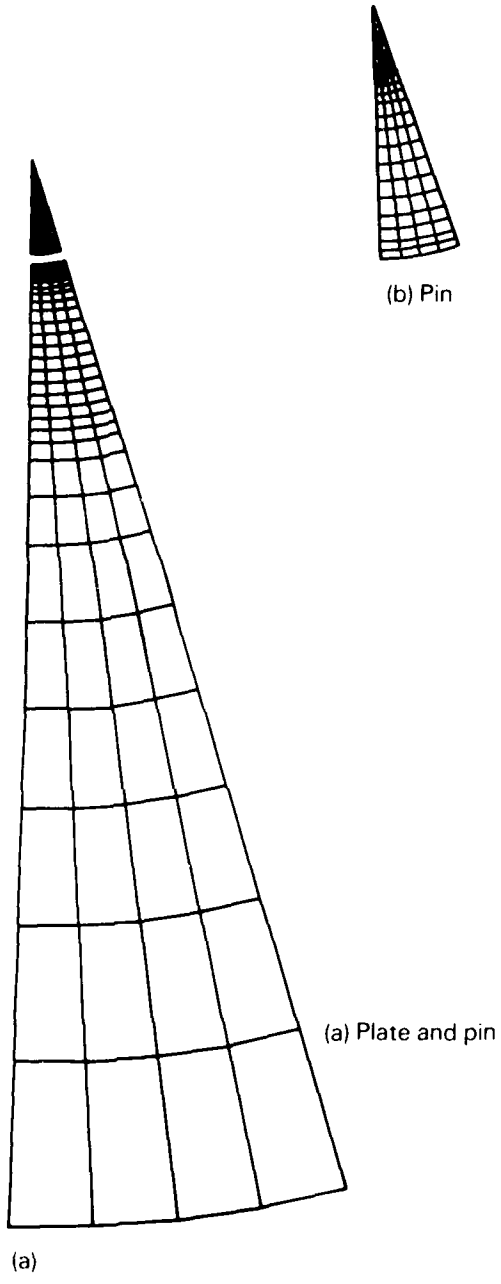

FIG. 1 FINITE ELEMENT MODEL OF PLATE AND PIN

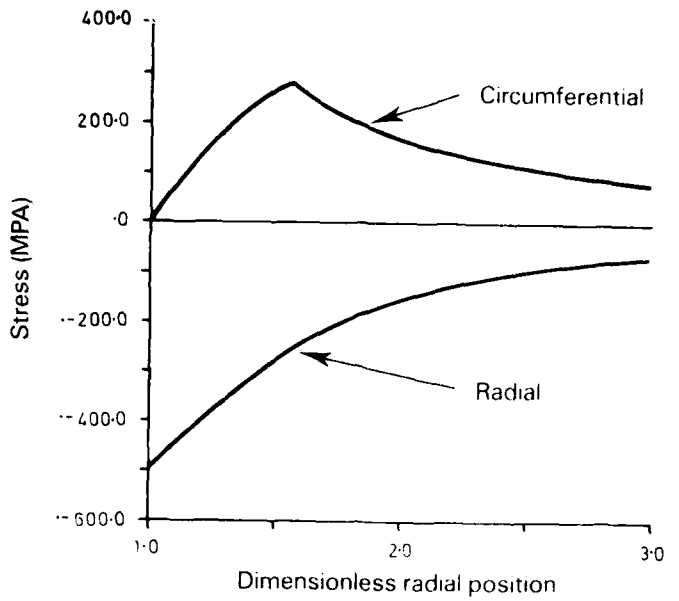

FIG. 2 CIRCUMFERENTIAL & RADIAL STRESSES IN PLATE 1.63% INTERFERENCE – PLANE STRESS.

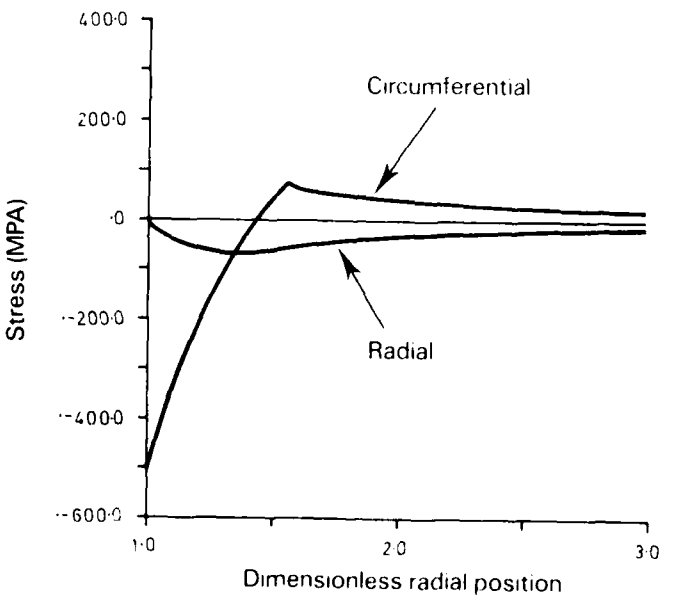

FIG. 3 CIRCUMFERENTIAL & RADIAL STRESSES IN PLATE UNLOADED FROM 1.63% INTERFERENCE – PLANE STRESS.

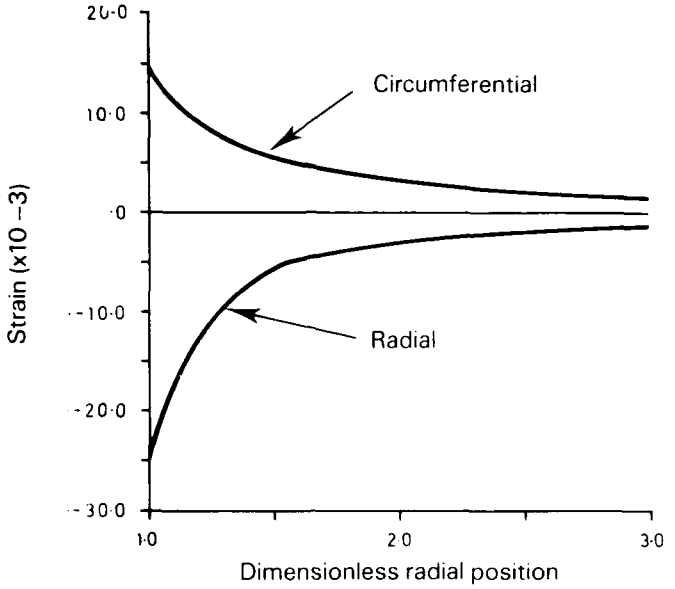

FIG. 4 CIRCUMFERENTIAL & RADIAL STRAINS IN PLATE 1.63% INTERFERENCE – PLANE STRESS.

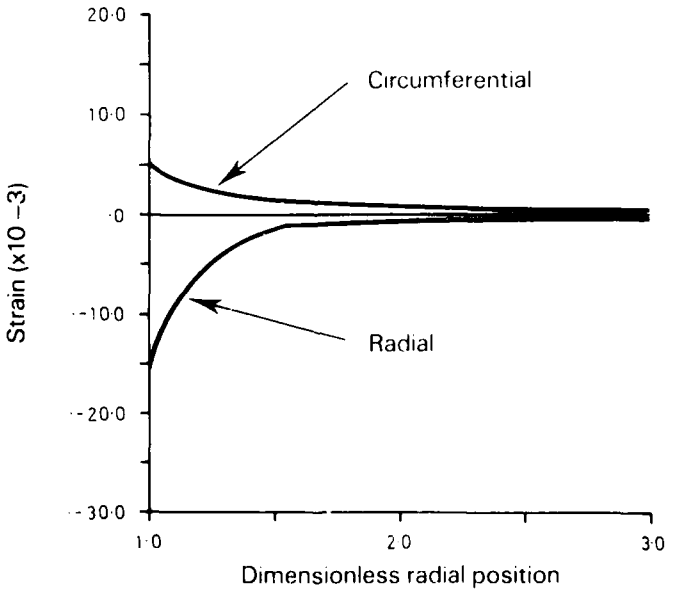

FIG. 5 CIRCUMFERENTIAL & RADIAL STRAINS IN PLATE UNLOADED FROM 1.63% INTERFERENCE – PLANE STRESS.

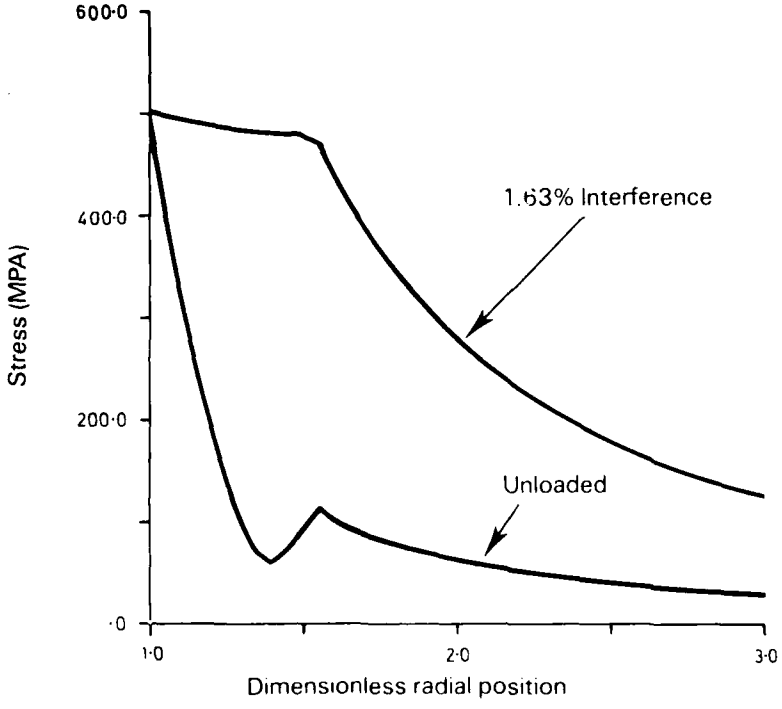

FIG. 6 VON MISES EQUIVALENT STRESSES
AT 1.63% INTERFERENCE AND UNLOADED – PLANE STRESS.

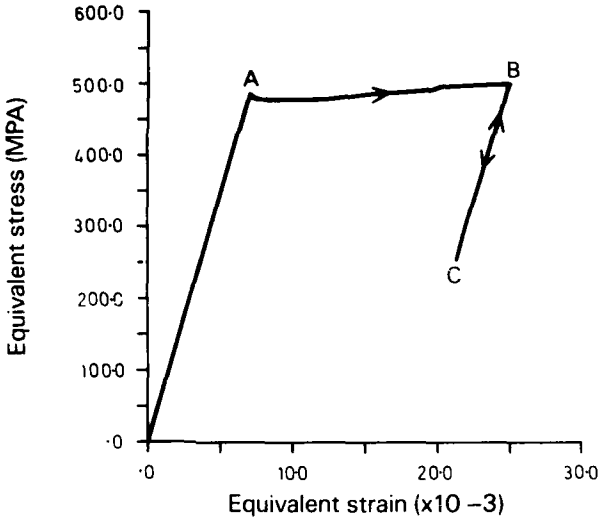

FIG. 7 EQUIVALENT STRESSES & STRAINS IN PLATE.

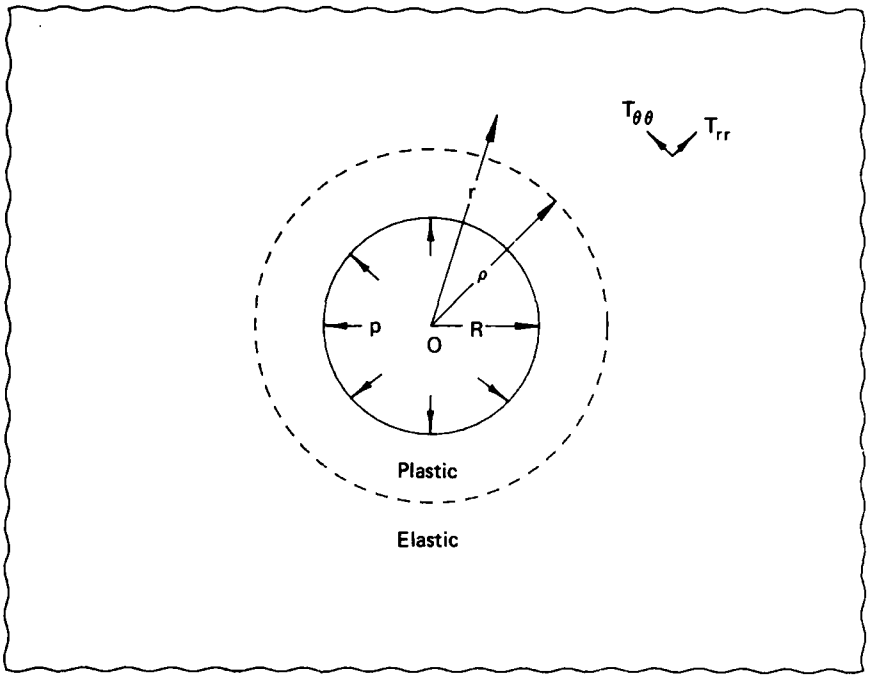

FIG. 8 HOLE IN INFINITE PLATE UNDER UNIFORM PRESSURE

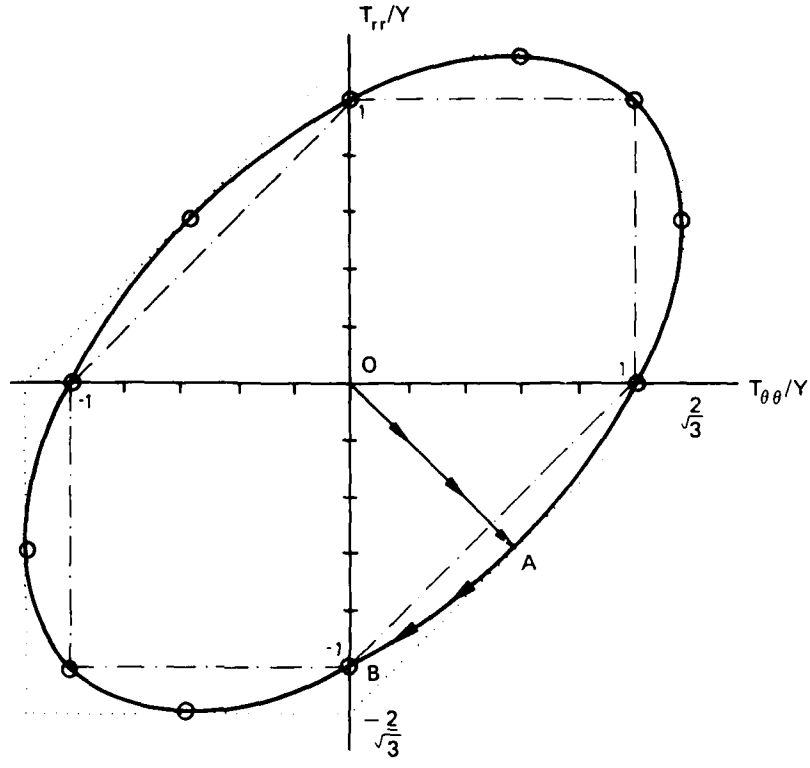

von Mises ——————

Tresca max. $|T_{\theta\theta} - T_{rr}|, |T_{\theta\theta}|, |T_{rr}| = Y$ — — — —

Tresca max. $|T_{\theta\theta} - T_{rr}|, |T_{\theta\theta}|, |T_{rr}| = \frac{2}{\sqrt{3}} Y$

Loading path (OAB) ——→

FIG. 9 COMPARISON OF YIELD CONDITIONS FOR PERFECTLY PLASTIC MATERIAL

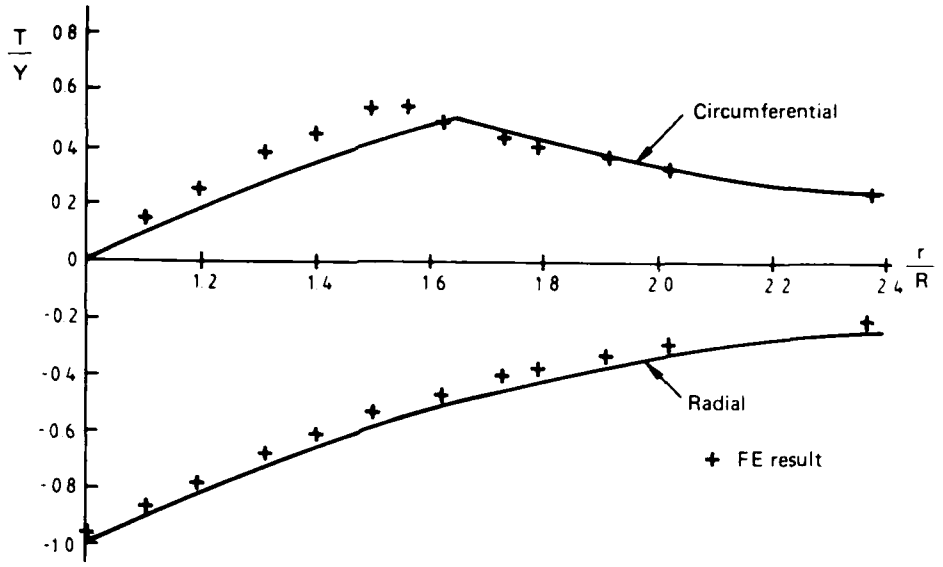

FIG. 10 COMPARISON OF ANALYTICAL AND FE STRESSES AT MAXIMUM LOAD

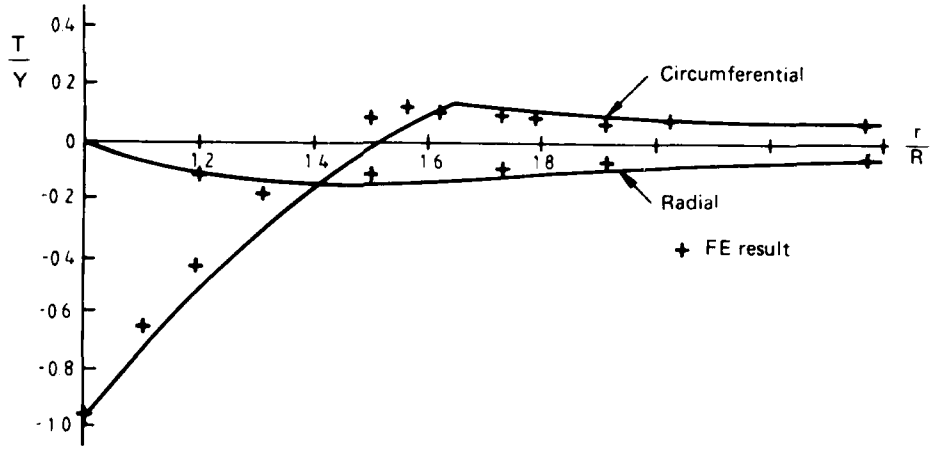

FIG. 11 COMPARISON OF ANALYTICAL AND FE RESIDUAL STRESSES

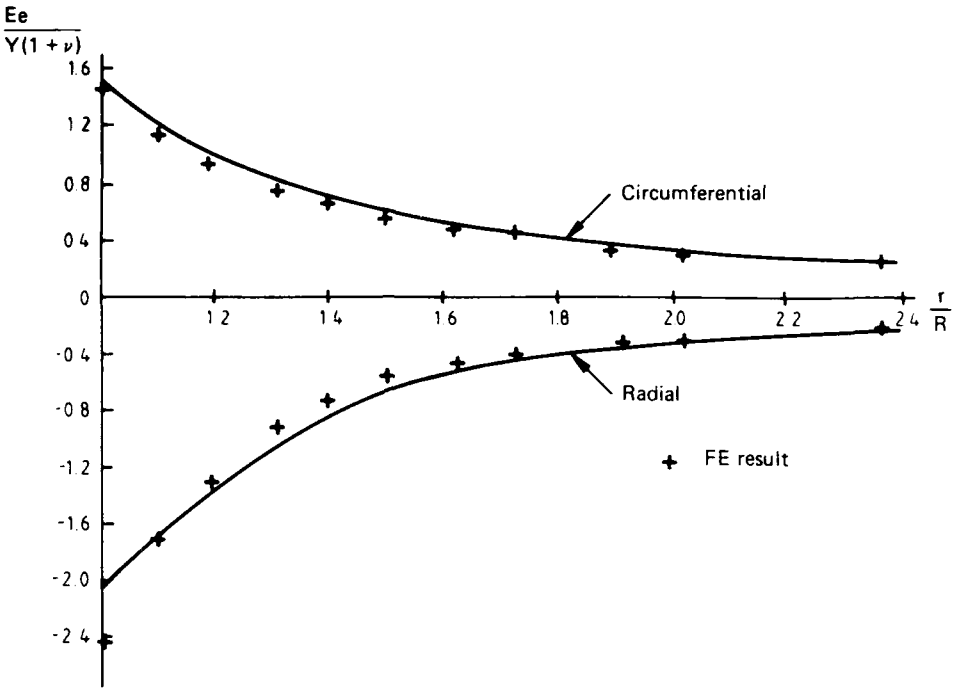

FIG. 12 COMPARISON OF ANALYTICAL AND FE STRAINS AT MAXIMUM LOAD

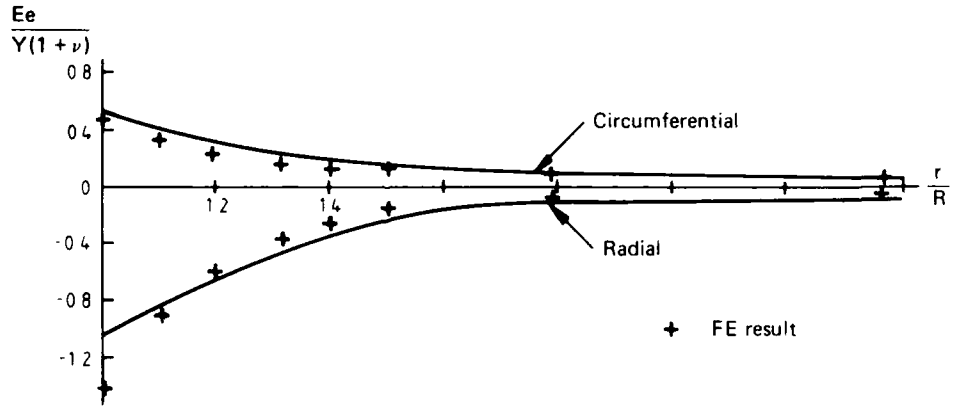

FIG. 13 COMPARISON OF ANALYTICAL AND FE RESIDUAL STRAINS

DISTRIBUTION

AUSTRALIA

Department of Defence

Defence Central
- Chief Defence Scientist
- Deputy Chief Defence Scientist (shared copy)
- Superintendent, Science and Program Administration (shared copy)
- Controller, External Relations, Projects and Analytical Studies (shared copy)
- Counsellor, Defence Science (London) (Doc Data Sheet Only)
- Counsellor, Defence Science (Washington) (Doc Data Sheet Only)
- S.A. to Thailand MRD (Doc Data Sheet Only)
- S.A. to the DRC (Kuala Lumpur) (Doc Data Sheet Only)
- OIC TRS, Defence Central Library
- Document Exchange Centre, DISB (18 copies)
- Joint Intelligence Organisation
- Librarian H Block, Victoria Barracks, Melbourne
- Director General - Army Development (NSO) (4 copies)
- Defence Industry and Material Policy, FAS

Aeronautical Research Laboratories
- Director
- Library
- Divisional File — Structures
- Authors: R. P. Carey
  B. C. Hoskin
- M. Heller
- R. Jones
- G. S. Jost
- J. Y. Mann
- J. Paul
- A. Wong

Materials Research Laboratories
- Director/Library

Defence Research Centre
- Library

RAN Research Laboratory
- Library

Navy Office
- Navy Scientific Adviser
- Director of Naval Aircraft Engineering
- Superintendent, Aircraft Maintenance and Repair

Army Office
- Scientific Adviser — Army
- Engineering Development Establishment Library
- Royal Military College Library

Air Force Office
Air Force Scientific Adviser
Aircraft Research and Development Unit
Library
Technical Division Library
Director General Aircraft Engineering — Air Force
HQ Support Commnand (SLENGO)
RAAF Academy, Point Cook

Central Studies Establishment
Information Centre

Department of Science
Bureau of Meteorology, Library

Department of Aviation
Library
Flight Standards Division

Statutory and State Authorities and Industry
Aerospace Technologies Australia
Manager
Library
Australian Nuclear Science and Technology Organisation
Australian Airlines, Library
Qantas Airways Limited
Ansett Airlines of Australia, Library
Hawker de Havilland Aust. Pty Ltd, Bankstown, Library

Universities and Colleges
Adelaide
Barr Smith Library

Flinders
Library

La Trobe
Library

Melbourne
Engineering Library

Monash
Hargrave Library

Newcastle
Library

Sydney
Engineering Library

NSW
Physical Sciences Library
Library, Australian Defence Force Academy

Queensland
Library

Tasmania
Engineering Library

Western Australia
Library

RMIT
Library

CANADA
CAARC Coordinator Structures
International Civil Aviation Organization, Library

NRC
Aeronautical & Mechanical Engineering Library

UNIVERSITIES AND COLLEGES
Toronto
Institute for Aerospace Studies

FRANCE
ONERA, Library

INDIA
CAARC Coordinator Structures
Defence Ministry, Aero Development Establishment, Library
Hindustan Aeronautics Ltd, Library
National Aeronautical Laboratory, Information Centre

INTERNATIONAL COMMITTEE ON AERONAUTICAL FATIGUE
per Australian ICAF Representative (25 copies)

ISRAEL
Technion-Israel Institute of Technology, Library

JAPAN
National Research Institute for Metals, Fatigue Testing Div.

UNIVERSITIES
Kagawa University
Professor H Ishikawa

NETHERLANDS
National Aerospace Laboratory (NLR), Library

NEW ZEALAND
Defence Scientific Establishment, Library

SWEDEN
Swedish National Research Institute (FOA)

SWITZERLAND
F + W (Swiss Federal Aircraft Factory)

UNITED KINGDOM
Ministry of Defence, Research, Materials and Collaboration
CAARC, Secretary

Royal Aircraft Establishment
Bedford, Library
Farnborough, Dr G Wood, Materials Department
Commonwealth Air Transport Council Secretariat

National Physical Laboratory, Library
National Engineering Laboratory, Library
CAARC Co-ordinator, Structures
Rolls-Royce Ltd, Aero Division Bristol, Library

British Aerospace
Kingston-upon-Thames, Library
Hatfield-Chester Division, Library

UNIVERSITIES AND COLLEGES

Bristol
Engineering Library

Cambridge
Library, Engineering Department

London
Professor G. J. Hancock, Aero Engineering

Nottingham
Science Library

Southampton
Library

Strathclyde
Library

Cranfield Inst. of Technology
Library

Imperial College
Aeronautics Library

UNITED STATES OF AMERICA
NASA Scientific and Technical Information Facility
Materials Information, American Society for Metals

Boeing Company, Library
Kentex Research Library
Lockheed-California Company
Lockheed Missiles and Space Company
Lockheed Georgia
McDonnell Aircraft Company, Library

UNIVERSITIES AND COLLEGES

Johns Hopkins
Professor S. Corrsin, Engineering

Iowa State
Dr G. K. Serovy, Mechanical Engineering

Iowa
Professor R. I. Stephens

Princeton
Professor G. L. Mellor

Massachusetts Inst. of Tech.
MIT Libraries

SPARES (10 copies)
TOTAL (161 copies)

AL 148
REVISED APRIL 87

DEPARTMENT OF DEFENCE

DOCUMENT CONTROL DATA

PAGE CLASSIFICATION
UNCLASSIFIED

PRIVACY MARKING
-

1a. AR NUMBER	1b. ESTABLISHMENT NUMBER	2. DOCUMENT DATE	3. TASK NUMBER
AR-004-517	ARL-STRUC-R-425	DECEMBER 1986	DST 83/005

4. TITLE
A FINITE ELEMENT PROCEDURE FOR INTERFERENCE-FIT AND COLD-WORKING PROBLEMS WITH LIMITED YIELDING

5. SECURITY CLASSIFICATION
(PLACE APPROPRIATE CLASSIFICATION IN BOX(S) IE. SECRET (S), CONFIDENTIAL (C), RESTRICTED (R), UNCLASSIFIED (U).)

DOCUMENT	TITLE	ABSTRACT
U	U	U

6. No. PAGES
32

7. No. REFS.
2

8. AUTHOR(S)
R. P. CAREY and B. C. HOSKIN

9. DOWNGRADING/DELIMITING INSTRUCTIONS
-

10. CORPORATE AUTHOR AND ADDRESS
AERONAUTICAL RESEARCH LABORATORIES
P.O. BOX 4331, MELBOURNE VIC. 3001

11. OFFICE/POSITION RESPONSIBLE FOR
SPONSOR -
SECURITY -
DOWNGRADING -
APPROVAL -

12. SECONDARY DISTRIBUTION (OF THIS DOCUMENT)
Approved for public release.

OVERSEAS ENQUIRIES OUTSIDE STATED LIMITATIONS SHOULD BE REFERRED THROUGH ASDIS, DEFENCE INFORMATION SERVICES BRANCH, DEPARTMENT OF DEFENCE, CAMPBELL PARK, CANBERRA, ACT 2601

13a. THIS DOCUMENT MAY BE ANNOUNCED IN CATALOGUES AND AWARENESS SERVICES AVAILABLE TO.....
No limitations

13b. CITATION FOR OTHER PURPOSES (IE. CASUAL ANNOUNCEMENT) MAY BE [ ] **UNRESTRICTED OR** [ ] **AS FOR 13a.**

14. DESCRIPTORS
Finite element analysis
Interference fit devices
Fasteners
Cold working
Plastic analysis

15. DRDA SUBJECT CATEGORIES
0089D
0046E

16. ABSTRACT

A procedure is described for performing finite element analysis on an annular plate containing an interference-fit pin or a cold-worked hole by prescribing interface displacements. Strain-hardening is permitted but unloading beyond reverse yielding is not allowed. The procedure is verified against a comparable internal pressure case. An analytical solution for an infinite plate of a perfectly plastic material is also included for comparative purposes.

PAGE CLASSIFICATION
UNCLASSIFIED
PRIVACY MARKING

THIS PAGE IS TO BE USED TO RECORD INFORMATION WHICH IS REQUIRED BY THE ESTABLISHMENT FOR ITS OWN USE BUT WHICH WILL NOT BE ADDED TO THE DISTIS DATA UNLESS SPECIFICALLY REQUESTED.

16. ABSTRACT (CONT.)

17. IMPRINT

AERONAUTICAL RESEARCH LABORATORIES, MELBOURNE

18. DOCUMENT SERIES AND NUMBER	19. COST CODE	20. TYPE OF REPORT AND PERIOD COVERED
STRUCTURES REPORT 425	24 1050	

21. COMPUTER PROGRAMS USED

PAFEC

22. ESTABLISHMENT FILE REF. (S)

23. ADDITIONAL INFORMATION (AS REQUIRED)